Redox Biology 46 (2021) 102102

Contents lists available at ScienceDirect

Redox Biology

journal homepage: www.elsevier.com/locate/redox

Connexin hemichannels regulate redox potential via metabolite exchange and protect lens against cellular oxidative damage

Yumeng Quan [a,b], Yu Du [b], Changrui Wu [b], Sumin Gu [b], Jean X. Jiang [b,*]

[a] Department of Ophthalmology, First Affiliated Hospital of Xi'an Jiaotong University, Xi'an, Shaanxi, China
[b] Department of Biochemistry and Structural Biology, University of Texas Health Science Center, San Antonio, TX, USA

ARTICLE INFO

Keywords:
Connexin
Hemichannel
Redox metabolite
Redox potential
Oxidative damage
Lens

ABSTRACT

Increased oxidative stress contributes to cataract formation during aging. Anterior epithelial cells are a frontline antioxidant defense system with powerful capacities to maintain redox homeostasis and lens transparency. In this study, we report a new molecular mechanism of connexin (Cx) hemichannels (HCs) in lens epithelial cells to protect lens against oxidative stress. Our results showed haploinsufficiency of Cx43 elevated oxidative stress and susceptibility to cataracts in the mouse lens. Cx43 HCs opened in response to hydrogen peroxide (H_2O_2) or ultraviolet radiation (UVR) in human lens epithelium HLE-B3 cells, and this activation contributed to a cellular protective mechanism against oxidative stress-induced apoptotic cell death. Furthermore, we found that Cx43 HCs mediated the exchange of oxidants and antioxidants in lens epithelial cells undergoing oxidative stress. These transporting activities facilitated a reduction of intracellular reactive oxygen species (ROS) accumulation and maintained the intracellular glutathione (GSH) level through the exchange of redox metabolites and change of anti-oxidative gene expression. In addition, we show that Cx43 HCs can be regulated by the intracellular redox state and this regulation is mediated by residue Cys260 located at the Cx43 C-terminus. Together, our results demonstrate that Cx43 HCs activated by oxidative stress in the lens epithelial cells play a key role in maintaining redox homeostasis in lens under oxidative stress. Our findings contribute to advancing our understanding of oxidative stress induced lens disorders, such as age-related non-congenital cataracts.

1. Introduction

The lens is an avascular and transparent organ in the anterior segment of the eye, which refracts and focuses light on the retina. Lenses are constantly exposed to oxidative environments, such as ultraviolet radiation (UVR), thus they are prone to oxidative damage [1,2]. Oxidative damage triggers apoptosis of lens epithelial cells located at the anterior, outmost region of the lens, and this type of damage is a major cellular basis for the initiation of non-congenital cataracts [3,4]. As an avascular organ, one of the major means for the lens to receive nutrients and antioxidants is through a microcirculatory system, a network of membrane channels that includes ion channels and connexin (Cx) channels that can form hemichannels (HCs) and gap junctions [5]. Unlike gap junctions that mediate cell-cell communication between adjacent cells, unopposed Cx HCs mediate the exchange of small molecules between the intracellular and extracellular environments [6]. Growing evidence supports that HCs function as a pathway for exchange of ions and small molecules and participate in paracrine and autocrine signaling in normal and pathological conditions [7,8]. Therefore, HCs in lens epithelial cells could be a potential transport portal for redox metabolic molecules that contribute to maintaining cellular redox homeostasis in the lens.

The ocular lens contains two major cell types: epithelial cells that form a single layer along the anterior lens surface, and fiber cells that make up the bulk of the lens organ. Since mature fiber cells lose their nuclei and organelles and lack *de novo* synthesis of proteins during differentiation, it is believed that epithelial cells contain most of the synthetic, metabolic, and active transport machinery in the lens [1]. Thus, lens epithelial cells are a likely candidate responsible for maintaining the anti-oxidative defense system. Three Cx isoforms have been identified in the mammalian lens, Cx43, Cx46, and Cx50, among which Cx43 and Cx50 are expressed in lens epithelial cells [1,9]. Cx mutations are a leading cause of human congenital cataracts [10]. It was reported that early stage cataract formation was observed in Cx43 knockout mice

* Corresponding author. Department of Biochemistry and Structural Biology, University of Texas Health Science Center, 7703 Floyd Curl Drive, San Antonio, TX, 78229-3900, USA.
E-mail address: jiangj@uthscsa.edu (J.X. Jiang).

https://doi.org/10.1016/j.redox.2021.102102
Received 8 July 2021; Received in revised form 10 August 2021; Accepted 11 August 2021
Available online 19 August 2021

[11]. The Cx43 Y17S mutation has previously been associated with cataracts in oculodentodigital syndrome [12]. The study by Lai et al. (2006) [13] also showed that the Y17S mutation in Cx43 reduces the activity of gap junctions and HCs in C6 cells compared to wild type (WT) Cx43. These observations postulate that Cx43 Y17S mutation-induced cataract formation is due to a partial loss of normal function of gap junctions and/or HCs.

UVR and H_2O_2 are two major causes of oxidative stress in lens [14]. In response to environmental radiation and oxidants, ROS accumulates excessively in lens cells, including epithelial cells and the superficial fiber cells, as well as the surrounding fluid like aqueous humor [15]. To tackle constant oxidative insults from the environment, the lens possesses one of the highest tissue level of reduced GSH (~4–6 mM) [16] and a complex antioxidant defense system including enzymatic antioxidants, such as superoxide dismutase (SOD), glutathione peroxidase (GPX), and catalase (CAT) [17]. In comparison, lens fiber cells have minimal capabilities of redox metabolism and require antioxidant substances provided by lens epithelial cells, such as GSH [18]. Thus, epithelial cells are essential for maintaining whole lens transparency and metabolic hemostasis, but how lens epithelial cells maintain redox homeostasis has remained largely elusive.

Previous evidence implied that the HCs might be involved in regulating survival or cell death by facilitating the transport of various redox metabolites, including GSH and ROS [19–23]. The critical role of GSH in maintaining lens redox homeostasis and transparency is well recognized [16,17,24]. Therefore, we hypothesize that Cx HCs play a critical role in the antioxidant defense system to maintain GSH homeostasis and redox state balance in the lens epithelium. Cxs are transmembrane proteins containing four transmembrane domains, two extracellular loops, one cytoplasmic loop, and cytosolic N- and C- termini [25]. The C-terminus of Cx43 is a target for various posttranslational modifications [26]. The potential intracellular redox related cysteine residues are located in the

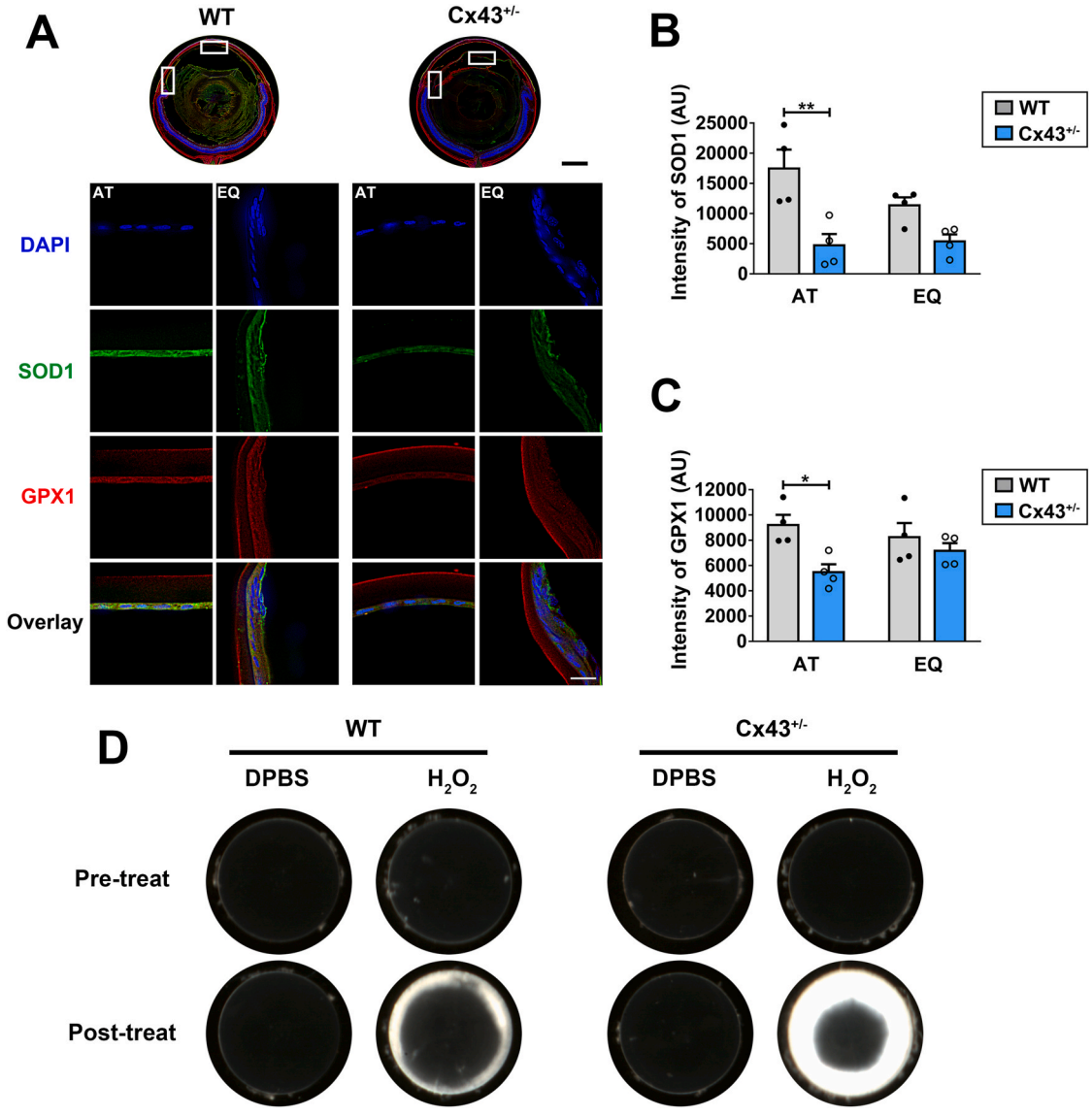

Fig. 1. Cx43 maintains the redox homeostasis of the ocular lens. (A) Cryosections of eyeballs from WT ($Cx43^{+/+}$) and $Cx43^{+/-}$ mice were immunostained with anti-GPX1 (red) or anti-SOD1 (green) antibody (upper panel). Scale bar = 500 μm. High resolution fluorescence images (lower panel) of anterior (AT) and equator (EQ) region of lenses are indicated by frames on whole cross-section images (corresponding upper panels). Scale bar = 20 μm. **(B and C)** The fluorescence signals of SOD1 **(B)** and GPX1 **(C)** positive areas were quantified by NIH ImageJ software. The data are presented as the mean ± SEM. (n = 4). *, $P < 0.05$; **, $P < 0.01$ (Unpaired T-test). **(D)** The lenses of WT and $Cx43^{+/-}$ mice were carefully dissected and kept transparent in culture media for 24 h at 37 °C before being treated with 0.5 mM H_2O_2. Photographic images were taken at the identical magnification using a dissecting microscope. (For interpretation of the references to colour in this figure legend, the reader is referred to the Web version of this article.)

C-terminus. It is believed that HCs are closed under physiological conditions. Recent studies have shown that the cellular redox potential changes, which occurs primarily at the Cx C-terminal region, can modify HC gating properties [27–29]. In addition, studies have shown that the changes of redox potential triggered by oxidative stress induce the opening of gap junctions and HCs [30–32]. UVR causes lens damages through the photochemical generation of ROS, including superoxide and its potent derivatives such as hydrogen peroxide, hydroxyl radicals, and singlet oxygen [33–36]. It is likely that the cellular redox alteration induced by UVR could be involved in the activation of HCs. However, it remains unclear how oxidative stress and UVR activate HCs and the role of redox potential alteration triggered by oxidative stress in the opening of HCs.

In this study, we found that HCs protect lens epithelial cells against oxidative stress by facilitating the influx/efflux of redox metabolic molecules such as, H_2O_2, oxidized glutathione (GSSG), and GSH. We further demonstrate that intracellular redox potential is critical for UVR-induced Cx43 HC opening and identify C260 as a unique redox sensory residue in Cx43.

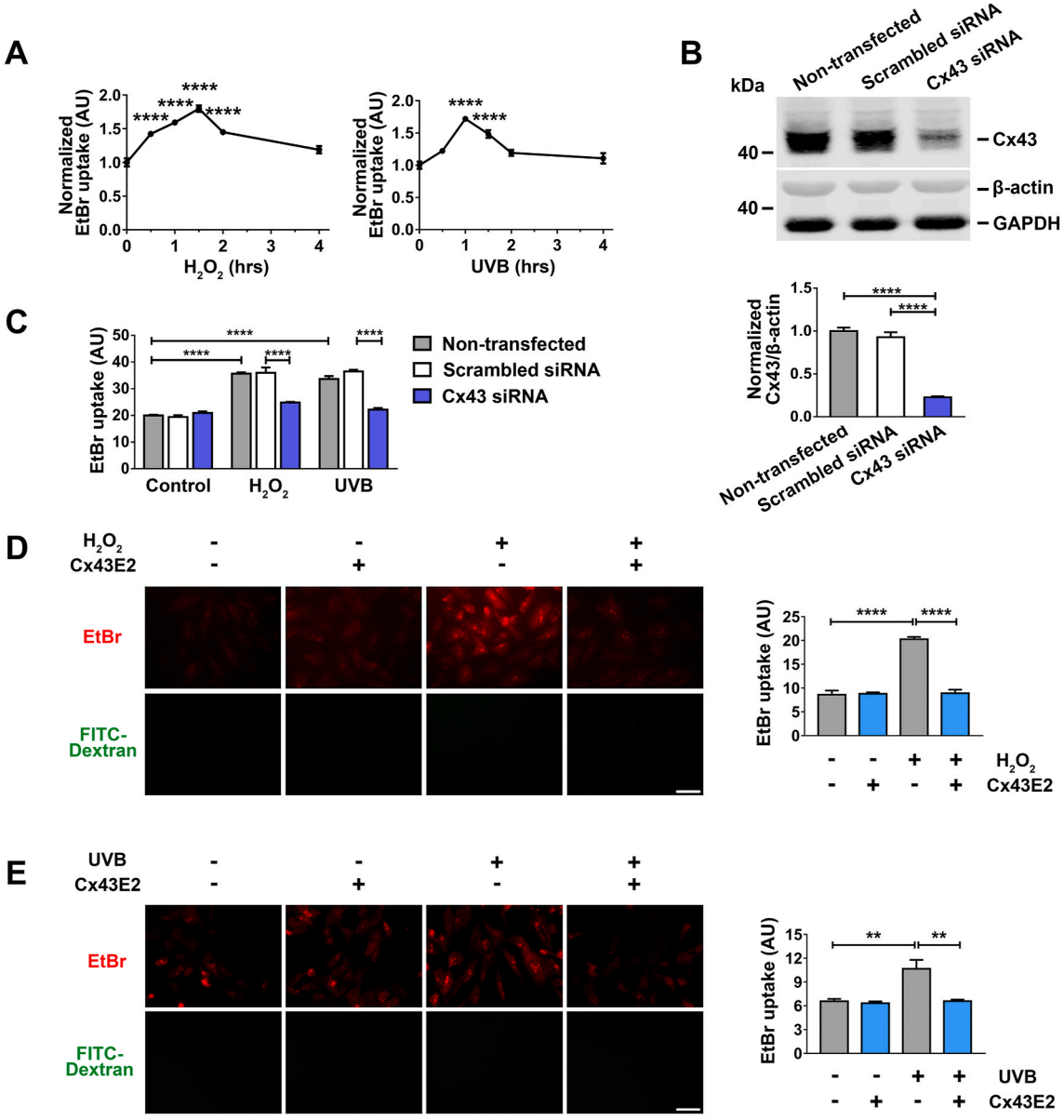

Fig. 2. Activation of Cx43 HCs in lens epithelial HLE-B3 cells by H_2O_2 and UVB radiation. (A) HLE-B3 cells were treated with 0.3 mM H_2O_2 or 63 mJ/cm^2 UVB radiation for different time periods and followed by a dye uptake assay with EtBr and FITC-Dextran. The data are presented as the mean ± SEM. (n = 3). ****, P < 0.0001 (One-way ANOVA). **(B)** HLE-B3 transfected with Silencer™ Negative Control or Cx43 siRNA. Membrane extracts were subjected to immunoblotted with anti-Cx43CT, β-actin and GAPDH antibodies. Lower panel shows the normalized ratios of band intensities of Cx43 and β-actin (n = 3). ****, P < 0.0001 (One-way ANOVA). **(C)** HLE-B3 cells were transfected with Silencer™ Negative Control or Cx43 siRNA by Lipofectamine RNAiMAX and then treated with 0.3 mM H_2O_2 or 63 mJ/cm^2 UVB radiation and followed by a dye uptake assay with EtBr and FITC-Dextran. The data are presented as the mean ± SEM. (n = 3). ****, P < 0.0001 (Two-way ANOVA). **(D and E)** HLE-B3 cells were treated with 0.3 mM H_2O_2 **(D)** for 1.5 h or 63 mJ/cm^2 UVB radiation **(E)** for 1 h Cx43E2 antibody was pre-incubated for 30 min before exposure of H_2O_2 or UVB radiation, and a dye uptake assay was performed with 0.1 mM EtBr and FITC-Dextran. The data are presented as the mean ± SEM. (n = 3). **, P < 0.01; ****, P < 0.0001 (One-way ANOVA). Scale bar: 50 μm. At least three microphotographs of fluorescence fields were taken under microscope (Keyence BZ-X710) with a 20X objective and TxRed and GFP filters. The average pixel density of 30 random cells was measured by using NIH ImageJ software.

2. Results

2.1. Downregulation of anti-oxidative protein expression in heterozygous Cx43-null ($Cx43^{+/-}$) mouse lens

Western blots showed that four month-old $Cx43^{+/-}$ lenses expressed less than half the amount of Cx43 compared to WT control (Fig. S1). We determined the level of oxidative stress markers in heterozygous Cx43-null mouse lens. Immunostaining with antibodies for oxidative stress markers, superoxide dismutase 1 (SOD1), and glutathione peroxidase 1 (GPX1) were used to evaluate the oxidative stress level (Fig. 1A). We found that in the heterozygous Cx43 knockout lens, reduced SOD1 and GPX1 levels were detected across various regions of the lens, especially at anterior and equatorial epithelial regions (Fig. 1A, lower panel). Moreover, the signals of SOD1 and GPX1 at anterior epithelium regions were significantly decreased in $Cx43^{+/-}$ lenses (Fig. 1B and C). Furthermore, we observed severer lens opacity in heterozygous Cx43-null mouse lens with H_2O_2 treatment compared to that in WT Cx43 lens (Fig. 1D). These results indicate that Cx43 may play a crucial role in regulating lens redox homeostasis, especially in the anterior epithelium.

2.2. Cx43 HCs in human lens epithelial cells are activated in response to H_2O_2 or UVB radiation

Cx HCs are closed under normal physiological conditions, and open in response to certain stimuli and cellular stress, such as, oxidative stress [19,20,23,28]. We used two major oxidative stress models, H_2O_2 and UVR, which are known to induce cataract formation in the lens [2,14]. HC activity was assessed in human lens epithelial cells (HLE-B3 cells) by ethidium bromide (EtBr) and FITC-dextran dye uptake. HCs are permeable to EtBr, while the larger FITC-dextran (~10 kDa) cannot pass through HCs and serve as a control for non-specific membrane permeability, including dying cells. Our results show that both H_2O_2 and UVB radiation treatment in HLE-B3 cells led to a drastic increase of EtBr uptake within the first 2 h and then gradually declined afterwards. This suggested that Cx HCs were activated rapidly in response to oxidative stress and UVB radiation (Fig. 2A). Noticeably, HC opening induced by UVB radiation was short-lived compared to that by H_2O_2. To determine the functional involvement of Cx43 in HLE-B3 cells, we knocked down cellular Cx43 expression by siRNA transfection (Fig. 2B). Quantification of dye uptake at 1 h and 1.5 h after H_2O_2 and UVB radiation treatment, respectively (the peak time point under oxidative stress), showed that HC activity was almost completely inhibited by Cx43 knockdown (Fig. 2C). We used Cx43E2 antibody, a specific Cx43 HC inhibitor [37],

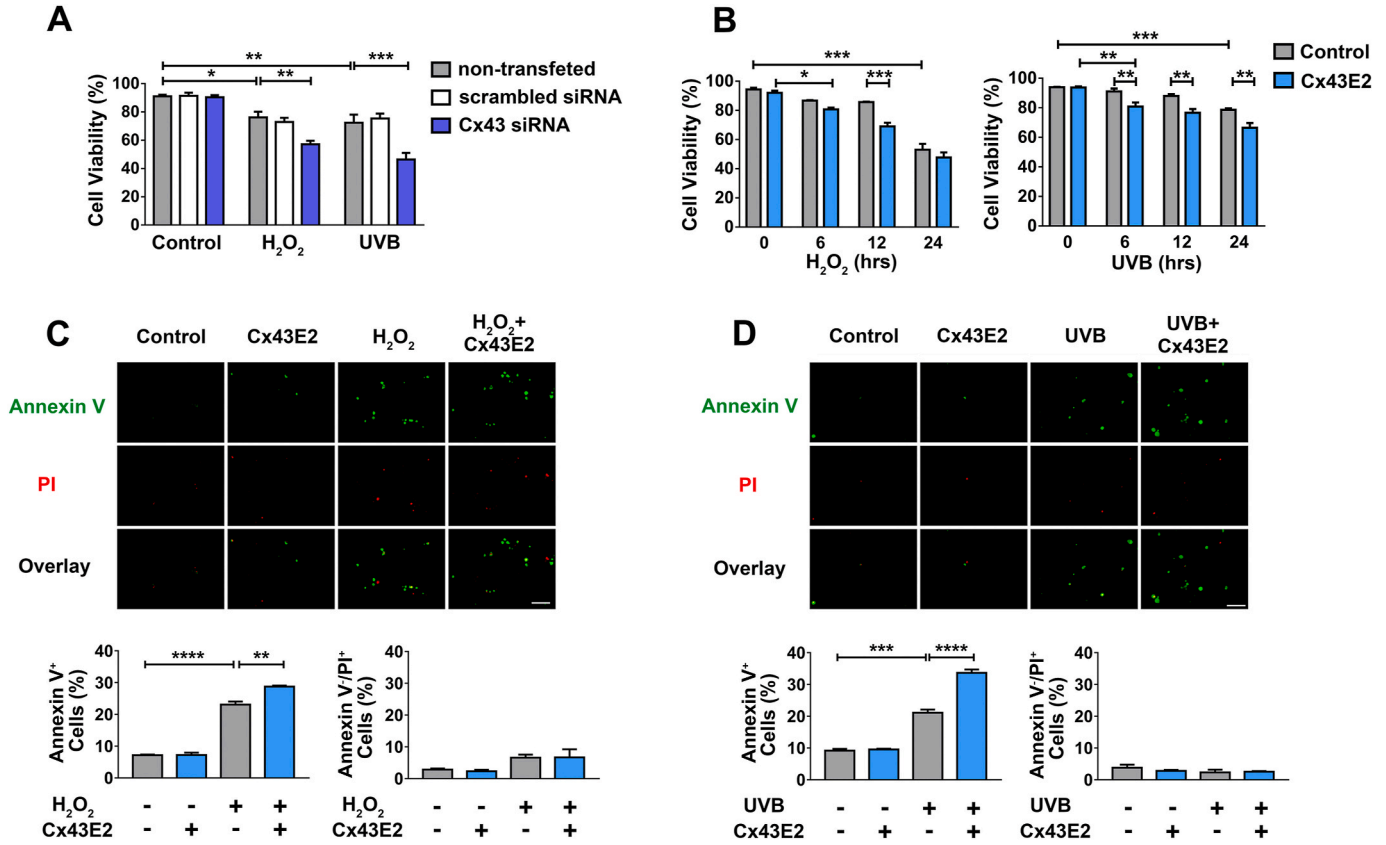

Fig. 3. Cx43 HCs protect lens epithelial HLE-B3 cells from H_2O_2 and UVB radiation-induced apoptosis. **(A)** HLE-B3 transfected with Silencer™ Negative Control or Cx43 siRNA were treated with 0.3 mM H_2O_2 or 63 mJ/cm^2 UVB radiation, and then subjected to a cell viability assay using trypan blue staining, and cell numbers were counted using Countess™ II FL automated cell counter. The data are presented as the mean ± SEM. (n = 3). *, $P < 0.05$; **, $P < 0.01$; ***, $P < 0.001$ (Two-way ANOVA). **(B)** HLE-B3 cells were treated with 0.3 mM H_2O_2 or 63 mJ/cm^2 UVB radiation for different time periods and Cx43E2 antibody was pre-incubated 30 min before treatment with H_2O_2 or UVB and followed by cell viability analysis. The data are presented as the mean ± SEM. (n = 3). *, $P < 0.05$; **, $P < 0.01$; ***, $P < 0.001$ (Two-way ANOVA). **(C and D)** Cells were incubated with Cx43E2 antibody 30 min before the treatment with 0.3 mM H_2O_2 for 12 h **(C)** or UVB for 6 h **(D)**, and were then subject to analysis using the Dead Cell Apoptosis Kit with FITC-Annexin V and PI (Molecular Probes). Apoptosis was quantified by counting Annexin V^+ cell population and necrosis was quantified by counting Annexin V^-/PI^+ cell population. At least ten microphotographs of fluorescence fields were taken under a microscope (Keyence BZ-X710) with a 10X objective, and phase-contrast, TxRed or GFP filter. Positive cells were quantified and shown as a percentage of total counted cells. The data are presented as the mean ± SEM. (n = 3). **, $P < 0.01$; ***, $P < 0.001$; ****, $P < 0.0001$ (One-way ANOVA). Scale bar: 100 μm. (For interpretation of the references to colour in this figure legend, the reader is referred to the Web version of this article.)

to assess the response of the Cx43 HCs to oxidative stress and UVB radiation in HLE-B3 cells. The EtBr uptake (Fig. 2D and E) after H_2O_2 or UVB radiation treatment was reduced in cells treated with Cx43E2, suggesting that the increase of membrane permeability is mediated by Cx43 HCs.

2.3. Cx HCs protect HLE-B3 cells from H_2O_2 and UVB radiation-induced apoptotic cell death

To determine the role of Cx43 under oxidative stress or UVB radiation, we knocked down Cx43 by siRNA in cells before treatment with H_2O_2 or UVB radiation. Cell viability was determined by a Trypan blue staining assay. The results showed that knocking down Cx43 increased the susceptibility of the cells to both H_2O_2 and UVB radiation-induced cell death (Fig. 3A), indicating the protective role of Cx43 in cells under oxidative stress. We further tested the role of Cx43 HCs in cell viability by treating HLE-B3 cells with H_2O_2 or UVB radiation with or without Cx43E2 antibody (Fig. 3B). The results from the Trypan blue staining assay showed that both H_2O_2 and UVB radiation treatment led to decreased cell viability over the time. However, the treatment with Cx43E2 antibody significantly decreased cell viability at 12 h after H_2O_2 treatment, or 6 h after UVB radiation. This indicated that inhibition of Cx43 HCs accelerated the process of H_2O_2 and UVB radiation-induced cell death.

In the ocular lens, previous studies support the notion that lens epithelial cells are responsible for the initiation of non-congenital cataract formation [3]. To elucidate whether Cx43 HCs modulate apoptosis in lens epithelial cells under oxidative stress or UVB radiation, Annexin V and PI staining was performed at 12 h after H_2O_2 treatment (Fig. 3C) or 6 h after UVB radiation (Fig. 3D). Results showed that both H_2O_2 and UVB radiation predominantly induced apoptotic cell death as opposed to necrotic cell death. Furthermore, it was observed that inhibition of HCs by Cx43E2 antibody resulted in increased apoptotic cell death compared to controls without Cx43E2 treatment. These observations suggest that HCs play a role in protecting cells from apoptotic cell death triggered by oxidative stress.

2.4. Cx HCs inhibit intracellular ROS accumulation and maintain intracellular GSH levels

Anterior epithelial cells are one of the major sites of GSH synthesis, which plays a critical role in regulating and maintaining the overall lens redox state [38]. To elucidate the role of epithelial Cx43, we knocked down Cx43 with siRNA in HLE-B3 cells and measured the intracellular ROS and GSH level using commercial fluorescence-based probes. The results showed that deletion of Cx43 led to increased intracellular ROS levels (Fig. S2A) and decreased intracellular GSH levels (Fig. S2B) at 4 h after H_2O_2 or UVB treatment, suggesting that Cx43 is involved in protecting HLE-B3 from cell death by scavenging intracellular ROS and preserving intracellular GSH. Interestingly, Cx43 HCs initially responded in an opposite manner to H_2O_2 and UVB radiation in regulating the intracellular redox state; intracellular ROS levels significantly increased

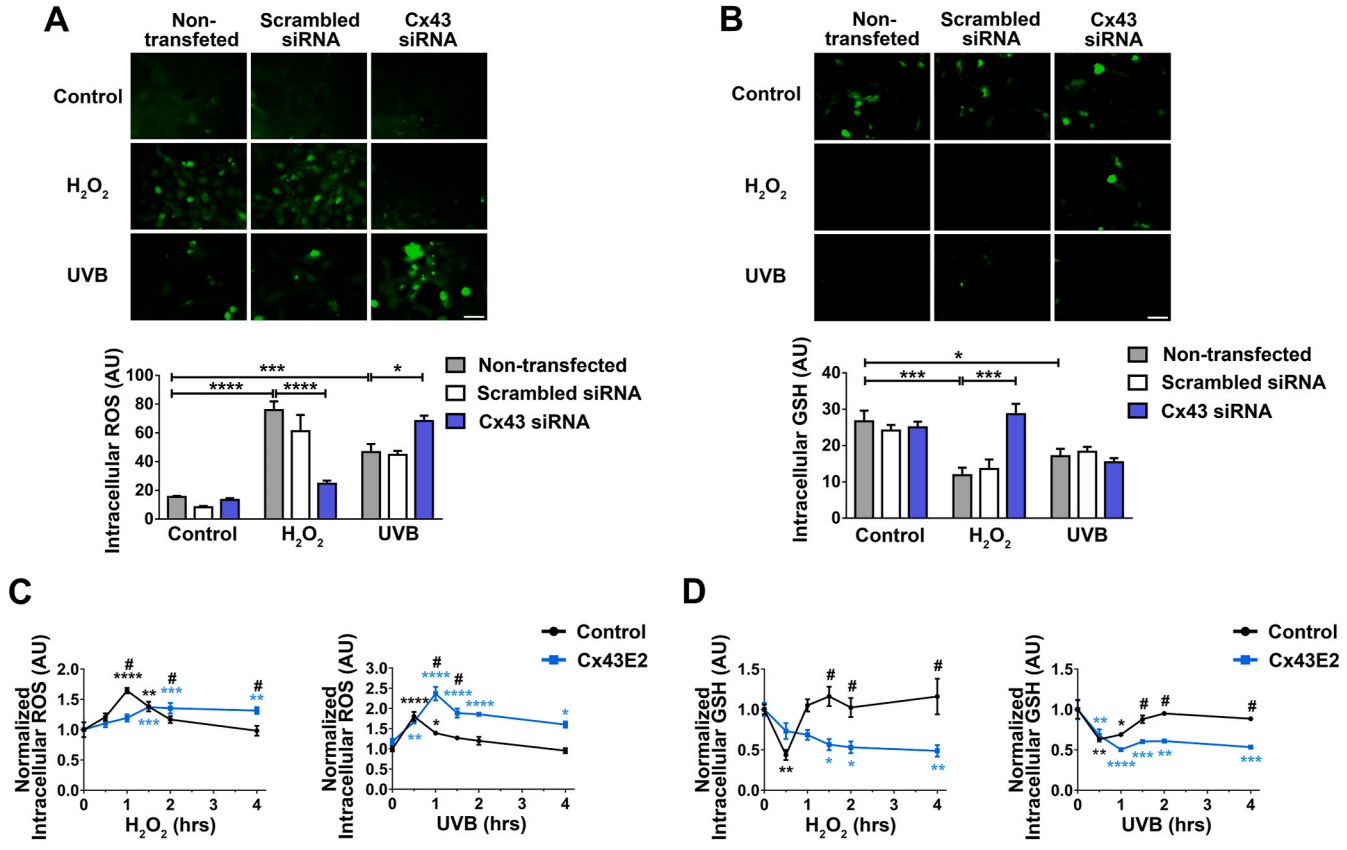

Fig. 4. Cx43 HCs reduce intracellular ROS accumulation and increase intracellular GSH level. (A and B) HLE-B3 transfected with Silencer™ Negative Control or Cx43 siRNA were treated with 0.3 mM H_2O_2 for 1 h or 63 mJ/cm^2 UVB radiation for 30 min. Intracellular ROS and GSH levels were detected by Carboxy-DCFDA **(A)** or Thioltracker™ **(B)** fluorescence, respectively. The data are presented as the mean ± SEM. (n = 3). *, $P < 0.05$; ***, $P < 0.001$; ****, $P < 0.0001$ (Two-way ANOVA). Scale bar: 50 μm. **(C and D)** HLE-B3 cells were pre-incubated with Cx43E2 antibody for 30 min before H_2O_2 treatment or UVB radiation for various time periods, and followed by incubating with 10 μM Carboxy-H_2DCFDA **(C)** or Thioltracker™ **(D)** for 30 min. The data are presented as the mean ± SEM. (n = 3). *, $P < 0.05$; **, $P < 0.01$; ***, $P < 0.001$; ****, $P < 0.0001$ compared to non-H_2O_2 or UVB treated control (Two-way ANOVA). #, $P < 0.05$ compared to without Cx43E2 antibody control group (Two-way ANOVA). At least three microphotographs of fluorescence fields were taken under a microscope (Keyence BZ-X710) using a 20X objective and a GFP filter. The average pixel density of 30 random cells was measured using NIH ImageJ software.

in Cx43 knockdown cells with UVB, while decreased in H_2O_2-treated cells as compared with non-transfected control cells (Fig. 4A). Moreover, compared with the redox state indicated by the ROS levels, the alteration of intracellular GSH level upon the treatment with H_2O_2 showed similar responses as that to the ROS levels, confirming the consistent cellular redox state (Fig. 4B). This consistence of redox state change, however, was not observed in the UVB radiation groups, a similar GSH level were detected in Cx43 WT and knockdown cells. These intriguing results raised a question regarding how Cx43 channels modulate intracellular ROS/GSH level in response to H_2O_2 and UVB.

We determined the intracellular ROS levels after H_2O_2 or UVB radiation treatment with or without Cx43E2 antibody after various time periods (Fig. 4C). Results showed that the intracellular ROS levels increased rapidly after H_2O_2 treatment and then restored to a normal level. In contrast, when the Cx43 was blocked by Cx43E2 antibody, the intracellular ROS levels accumulated slowly over time and continued to stay at a higher level (Fig. 4C, left panel). Similarly, UVB radiation also induced rapid increase of intracellular ROS levels and returned to baseline by 4 h. The similar persistent elevated ROS levels were seen in cells treated with Cx43E2 antibody (Fig. 4C, right panel). We also determined the intracellular ROS levels at 1 h and 3 h after H_2O_2 or UVB radiation treatment. With the presence of Cx43E2 antibody, an opposite change of intracellular ROS levels was observed at 1 h between H_2O_2 and UVB radiation-treated groups (Fig. S3, A and B).

We also assessed the intracellular GSH level in cells upon the same treatment (Fig. 4D). Results showed that both H_2O_2 and UVB irradiation led to an initial decrease of the GSH levels in response to oxidative stress and the GSH level was restored within 1–2 h. Consistent with ROS responses, GSH level in Cx43E2-treated cells were continuously lowered with time. Therefore, the time course study with H_2O_2 and UVB with Cx43E2 antibody suggests the critical role of Cx43 HCs in regulating intracellular ROS and GSH level and further implies that the protective role of Cx43 HCs against apoptotic death is likely mediated through increased intracellular GSH and reduced ROS.

2.5. *Cx HCs are involved in transient increase of cellular H_2O_2 and excretion of oxidized glutathione*

As shown in Fig. 3, after H_2O_2 treatment, intracellular ROS levels in Cx43E2 antibody treated cells accumulated slowly over time, contrary to a sharp increase observed in the control group. However, unlike the slow accumulation of ROS upon H_2O_2 stimulation in cells with inhibition of Cx43 HCs, this sharp, early increase was intensified under UVB radiation by Cx43E2 antibody treatment. We hypothesized that

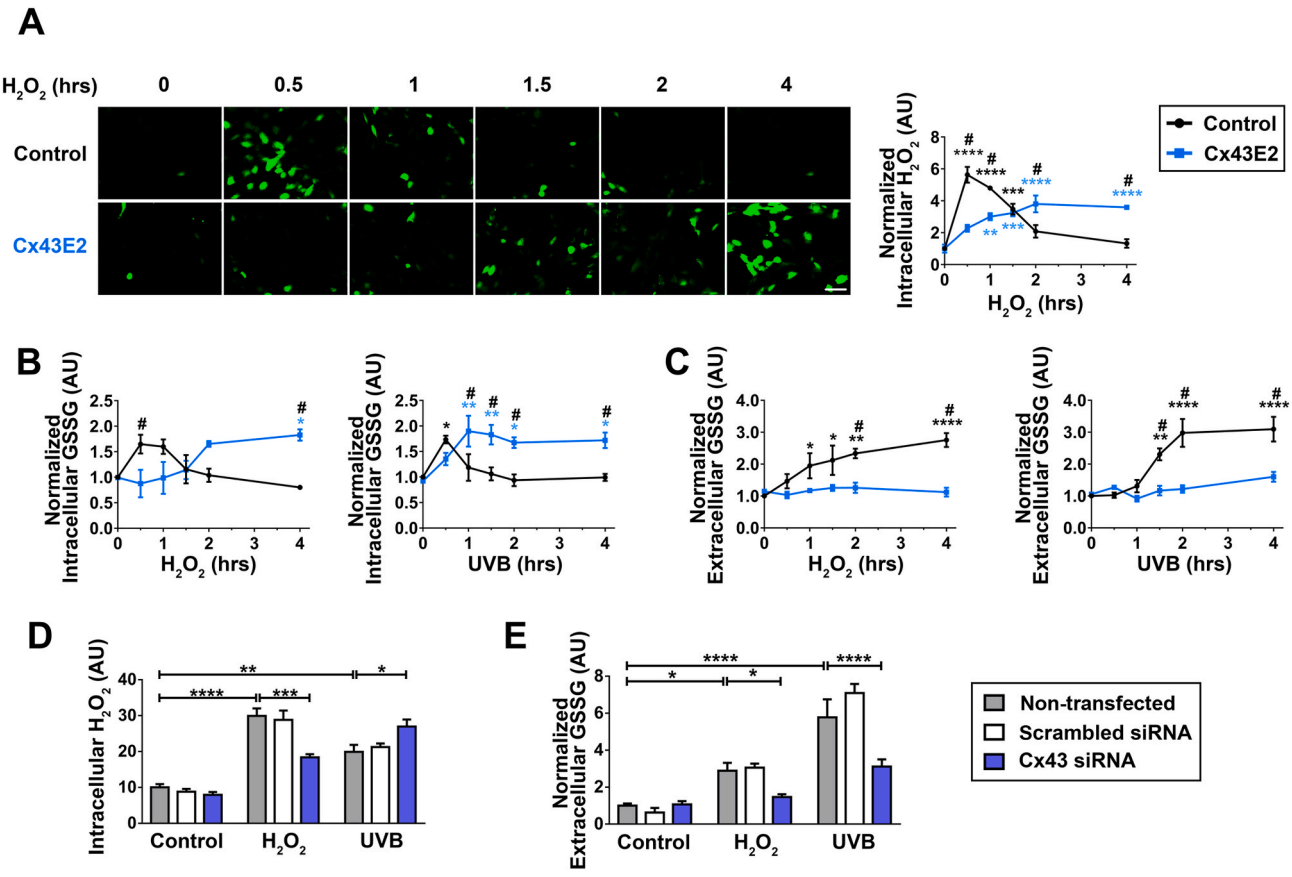

Fig. 5. Cx43 HCs mediate cellular uptake of H_2O_2 and excretion of oxidized glutathione. **(A)** Cells were pre-incubated with Cx43E2 antibody for 30 min and labeled with fluorescent Peroxide Sensor (Sigma-Aldrich) before the treatment with 0.3 mM H_2O_2 for various time periods. The intracellular H_2O_2 level was quantified by fluorescence intensity using NIH ImageJ software. The data are presented as the mean ± SEM. (n = 3). **, $P < 0.01$; ***, $P < 0.001$; ****, $P < 0.0001$ compared to non-H_2O_2 treated control (Two-way ANOVA). #, $P < 0.05$ compared to without Cx43E2 antibody control group (Two-way ANOVA). At least one microphotograph of fluorescence fields was taken under a 20X microscope (Keyence BZ-X710) using GFP filter. Scale bar: 50 μm. **(B and C)** HLE-B3 Cells pre-incubated with Cx43E2 antibody 30 min were treated with 0.3 mM H_2O_2 or UVB radiation for various time periods and intracellular and extracellular GSSG levels were tested using GSH/GSSG Ratio Detection Assay Kit (Fluorometric-Green, Abcam, ab138881). The data are presented as the mean ± SEM. (n = 3). *, $P < 0.05$; **, $P < 0.01$; ****, $P < 0.0001$ compared to non-H_2O_2 or UVB treated control (Two-way ANOVA). #, $P < 0.05$ compared to without Cx43E2 antibody control group (Two-way ANOVA). **(D and E)** HLE-B3 cells were transfected with Silencer™ Negative Control or Cx43 siRNA and then treated with 0.3 mM H_2O_2 or 63 mJ/cm^2 UVB radiation. The intracellular H_2O_2 level was quantified by measuring fluorescence intensity, and the extracellular GSSG level were tested using GSH/GSSH Ratio Detection Assay Kit. The data are presented as the mean ± SEM. (n = 3). *, $P < 0.05$; **, $P < 0.01$; ***, $P < 0.001$; ****, $P < 0.0001$ compared to non-treated control (Two-way ANOVA). (For interpretation of the references to colour in this figure legend, the reader is referred to the Web version of this article.)

inhibition of HCs by Cx43E2 antibody blocked accumulation of H_2O_2, thus inhibiting the rapid increase of ROS levels. To test this hypothesis, we performed an H_2O_2 uptake assay to determine the ability of HCs in mediating H_2O_2 influx. Results showed that HC inhibition led to a significant delay of intracellular H_2O_2 uptake compared to control cells with functional HCs (Fig. 5A), indicating the role of HCs in the increase of intracellular H_2O_2. Comparing intracellular H_2O_2 level at 30 min, H_2O_2 treatment exhibited a greater increase than UVB radiation (Fig. S3C). After initial increase, the H_2O_2 level rapidly declined in non-treated cells, but not in cells with impaired HCs.

In the cellular anti-oxidative system, H_2O_2 can be metabolized by GPX, while oxidized GSH (also known as glutathione disulfide, GSSG) can be reduced and converted back to GSH by glutathione-disulfide reductase (GSR), which forms a GSH redox cycle [16]. The capability of cells to reduce GSSG to GSH may be overwhelmed during severe oxidative damage, leading to an accumulation of intracellular GSSG, which promotes cataract formation [16,39]. The cellular redox level is indicated through the ratio of reduced GSH and oxidized GSSG. Although GSSG can be reduced to GSH by enzymes, GSSG might be actively transported out of the cell within a short time to maintain balance in the GSH redox cycle. Here we measured intracellular (Fig. 5B) and extracellular (Fig. 5C) level of GSSG to determine the role of HCs in mediating GSSG efflux. The intracellular GSSG level increased rapidly in response to H_2O_2 and UVB radiation treatment, and was then restored to a normal level. When Cx43 HCs were blocked by Cx43E2 antibody, the intracellular GSSG level accumulated slowly over time and was maintained at a higher level. The time-dependent changes of GSSG after H_2O_2 or UVB radiation treatment with or without functional HCs were in good agreement with those of intracellular ROS levels, suggesting an overall consistent oxidative state in cells. Importantly, after H_2O_2 or UVB radiation treatment, we observed increased extracellular GSSG level in cells and this increase was not observed in cells with inhibited HCs, indicating that HCs mediate GSSG export under oxidative stress.

We further validated the capability of Cx43 in regulating intracellular H_2O_2 and GSSG levels in Cx43 knockdown cells (Fig. 5D and E). Cx43 was knocked down by siRNA and scrambled siRNA was used as a control. A decrease of intracellular H_2O_2 level was observed after H_2O_2 treatment in Cx43 knockdown cells when compared to non-transfected and scrambled siRNA H_2O_2-treated controls, while UVB exposure showed an increase in intracellular H_2O_2 level in Cx43 knockdown cells. In addition, after H_2O_2 treatment or UVB irradiation, we observed a decline in extracellular GSSG level in cells with Cx43 knockdown when compared to their respective treated controls. These results further confirm the role of Cx43 HCs in mediating intracellular H_2O_2 level and GSSG efflux under oxidative stress.

2.6. Cx43 HC activation alters anti-oxidative gene expression in response to oxidative stress

We hypothesized that the elevated ROS levels in response to H_2O_2 uptake triggers the increase of anti-oxidative gene expression. Quantitative PCR and western blots were performed to assess anti-oxidative gene/protein expression under oxidative stress. We determined glutathione peroxidase 1 (GPX1), glutathione peroxidase 8 (GPX8), glutathione-disulfide reductase (GSR), glutathione S-transferase Mu 2 (GSTM2), microsomal glutathione S-transferase 1 (MGST1), superoxide dismutase 1 (SOD1), and heme oxygenase 1 (HMOX1) gene expression with or without Cx43E2 antibody after H_2O_2 or UVB radiation treatment (Fig. 6A and B, S4, A-E). Among these anti-oxidative genes, SOD1 and GPX1 showed the most significant changes. Results from qPCR showed that H_2O_2 treatment in HLE-B3 cells led to a time-dependent, yet rapid and significant increase of GPX1 and SOD1 mRNA levels (Fig. 6A), indicating the activation of cellular anti-oxidative mechanism. After UVB irradiation, we observed instead an initial decrease of mRNA levels of GPX1, and SOD1 (Fig. 6B). The response to UVB was opposite to H_2O_2-treated cells, suggesting that H_2O_2 treatment and UVB irradiation triggered anti-oxidative responses through different mechanisms. Consistent with gene expression, results from western blot showed opposite changes in levels of anti-oxidative proteins, GPX1 and SOD1; increased upon H_2O_2 treatment while decreased upon UVB radiation treatment. Nevertheless, these changes were abolished in cells treated with Cx43E2 antibody (Fig. 6, A-C), suggesting that HCs play an essential role in regulating anti-oxidative genes likely through intracellular H_2O_2 and ROS.

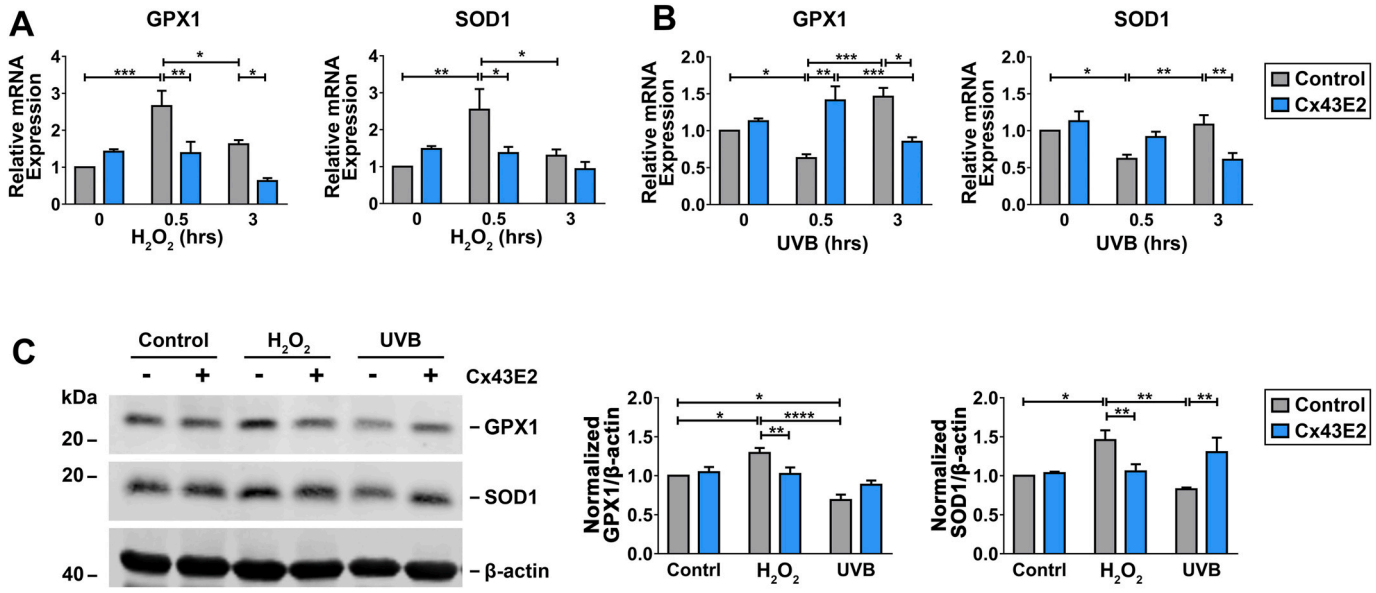

Fig. 6. Inhibition of Cx43 HCs alters anti-oxidative gene expression in response to oxidative stress. (A and B) The cells were pre-incubated with or without Cx43E2 antibody for 30 min followed by incubation with 0.3 mM H_2O_2 **(A)** or 63 mJ/cm^2 UVB radiation **(B)** for 0, 0.5, and 3 h. RNA extracts were prepared and subjected to qRT-PCR analysis for GPX1 or SOD1 mRNA expression. **(C)** HLE-B3 cells were pre-incubated with or without Cx43E2 antibody for 30 min followed by incubation with 0.3 mM H_2O_2 or 63 mJ/cm^2 UVB radiation and immunoblotting with anti-GPX1, SOD1 or β-actin antibody. The protein levels of SOD1 and GPX1 were quantified by Image Studio Site software (LI-COR Biosciences). The data are presented as the mean ± SEM. (n = 3). *, P < 0.05; **, P < 0.01; ***, P < 0.001; ****, P < 0.0001 (Two-way ANOVA).

2.7. Cx HCs mediate glutathione uptake and protect cells against oxidative stress

Lens epithelial cells located at the anterior surface of the lens face the aqueous humor, which provides reductants and nutrition, and removes metabolic products, thus contributing to lens homeostasis [40]. The aqueous humor is postulated as a potential source of GSH for lens epithelial cells, and Cx HCs are permeable to GSH [18,41,42]. To determine the GSH transport activity of HCs, we performed GSH uptake assays using Thioltracker™, a probe detecting the reducing state of thiols in the cell. The intracellular GSH level was significantly elevated after H_2O_2 or UVB radiation treatment in the presence of exogenous GSH, suggesting an active uptake of extracellular GSH in response to oxidative stress. This increase, however, was diminished in cells treated with Cx43E2 antibody (Fig. 7A). Cellular apoptosis analysis showed that exogenous GSH treatment reduced apoptotic death induced by H_2O_2 or UVB radiation, and such reduction by GSH was attenuated by HC inhibition by Cx43E2 antibody (Fig. 7B). These results together indicated that the protective role of HCs against oxidative stress is mediated through the influx of GSH.

2.8. Cx43 HC activity is regulated by the intracellular redox state

Several studies reported that HCs are regulated by redox-related alterations, like oxidants or reducing molecules [27–29] and the extracellular or intracellular cysteine residue on Cx43 could be potential sensory residues for intracellular redox potential [43]. We first determined if extracellular or intracellular domains of Cx43 were redox sensory regions by using two reducing reagents GSH and DTT at various time points during UVB radiation (Fig. 8A, right lower panel). DTT is permeable to the lipid bilayer while GSH does not permeate the membrane. Pre-treatment of GSH followed by UVB radiation did not affect EtBr uptake (Fig. 8A), suggesting that the extracellular reducing environment did not affect HC activation. However, when cells were incubated with GSH after UVB radiation, HC activation was significantly inhibited, indicating entry of GSH with the increased intracellular reducing state could suppress HC activity. A similar inhibition of HC opening induced by UVB radiation was obtained in cells pre-treated or

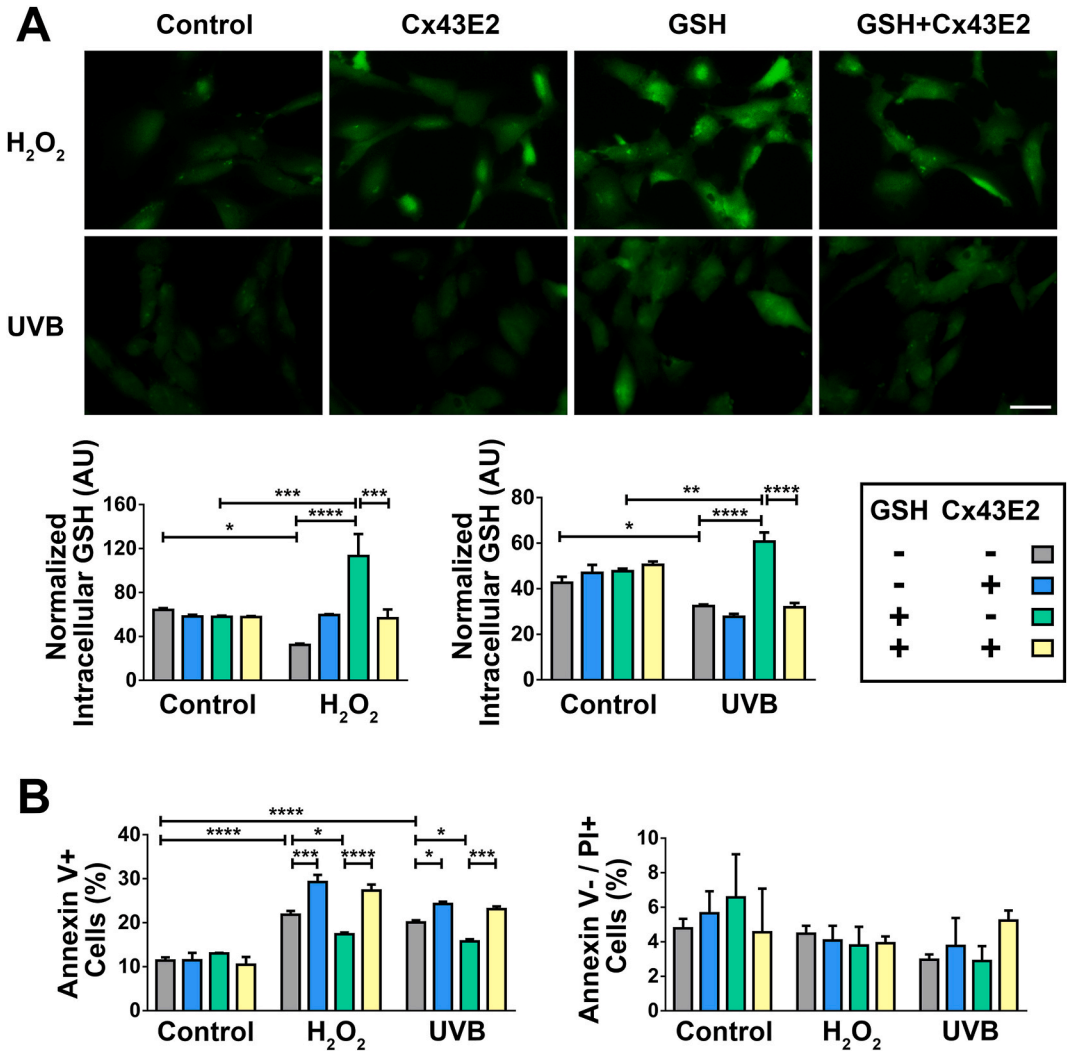

Fig. 7. Cx43 HCs mediate glutathione uptake and protect cells against oxidative stress. (A) Cells pre-treated with Cx43E2 antibody for 30 min were incubated 1 mM GSH for 20 min before treatment with H_2O_2 or UVB radiation. The cells were then incubated with fluorescent Thioltracker™ and the intracellular GSH level was quantified by measuring fluorescence intensity. At least three microphotographs of fluorescence fields were taken under a 20X microscope (Keyence BZ-X710) using a GFP filter. Bar, 50 μm. The average pixel density of 30 random cells was measured by using NIH ImageJ software. **(B)** Cells pre-treated with Cx43E2 antibody for 30 min were incubated 1 mM GSH for 20 min before treatment with H_2O_2 or UVB radiation, and followed by incubation with the Dead Cell Apoptosis Kit with FITC–Annexin V and PI (Molecular Probes). The cells with positive signal were quantified and presented as a percentage of total counted cells. Apoptosis (left panel) was quantified by counting Annexin V^+ cell population; Necrosis (right panel) was quantified by counting Annexin V^-/PI^+ cell population. The data are presented as the mean ± SEM. (n = 3). *, $P < 0.05$; ***, $P < 0.001$; ****, $P < 0.0001$ (Two-way ANOVA).

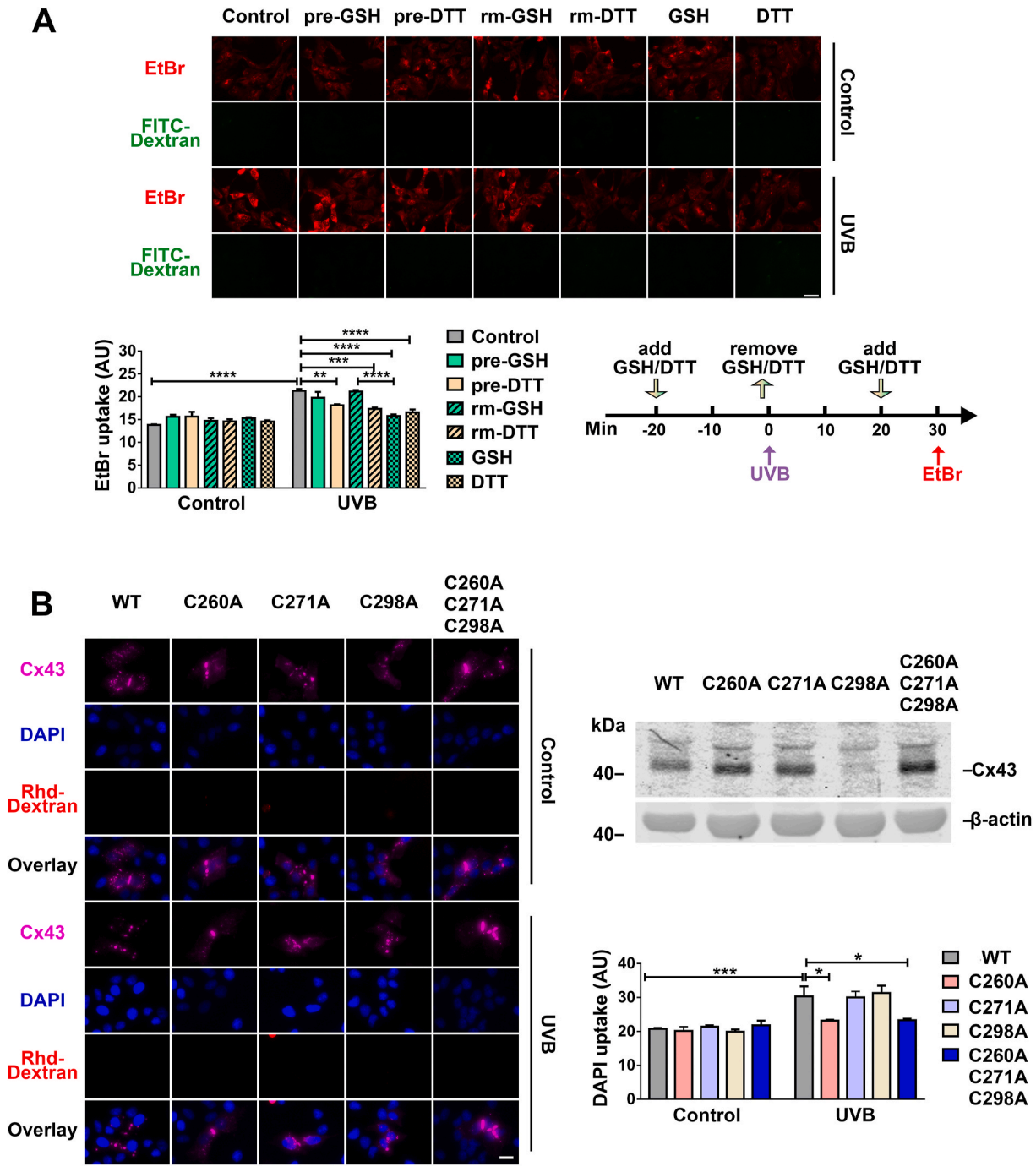

Fig. 8. Cx43 HC activity is regulated by intracellular redox state. (A) HLE-B3 cells were treated with or without 63 mJ/cm^2 UVB radiation and followed by a dye uptake assay with EtBr and FITC-Dextran. Cells were pre-treated with GSH or DTT (indicated as pre-GSH or pre-DTT) for 20 min and followed by replacing with culture medium collected from parallel cells cultured for the same time periods immediately before UVB radiation (indicated as rm-GSH or rm-DTT). After UVB radiation, 1 mM GSH or DTT (indicated as GSH or DTT) were added and incubated for 10 min before EtBr uptake assay. Scale bar: 50 μm. **(B)** HeLa cells expressing WT Cx43 or various Cx43 cysteine mutants and treated with or without 108 mJ/cm^2 UVB radiation, were incubated with DAPI and rhodamine-dextran for 5 min then immunostained with anti-Cx43CT (purple) antibody. Scale bar: 20 μm. Membrane extracts were prepared and then immunoblotted with anti-Cx43 antibody (upper right panel). At least three microphotographs of fluorescence fields were taken under a microscope (Keyence BZ-X710) with 20X objective and TxRed, Cy5 or DAPI filters. The average pixel density of 30 random cells was measured by using ImageJ software. The data are presented as the mean ± SEM. (n = 3). *, $P < 0.05$; **, $P < 0.01$; ***, $P < 0.001$; ****, $P < 0.0001$ (Two-way ANOVA). (For interpretation of the references to colour in this figure legend, the reader is referred to the Web version of this article.)

post-treated with DTT. Contrary to GSH, we observed slightly inhibited HCs activation even when cells were pre-treated with DTT due to the membrane permeable property of this reductant. These data suggested that intracellular reducing states negatively regulate HC activation. Moreover, this study indicates that the redox sensory residues are likely to be located in the cytoplasmic domain of Cx43.

Given that cysteine residues in proteins are common redox sensory residues, we introduced various site mutant forms of Cx43 into HeLa cells and determined HC activation upon UVB radiation. We made single or triple site mutation by replacing cytosolic cysteine's C260A, C271A,

and C298A of Cx43 with alanine (Fig. 8B, right upper panel) and assessed HC activity using the DAPI uptake assay (Fig. 8B). Results showed that a mutation at residue C260 resulted in significantly reduced HC activation. This result suggests that residue C260 at the Cx43 C-terminus is a likely intracellular redox sensor that regulates HC activation in response to the cellular redox state.

3. Discussion

Due to lack of blood vessels, the lens is postulated to obtain nutrients and antioxidants by diffusion from surrounding fluids, and/or through a microcirculatory system based on a network of channels, including gap junction channels [5,44]. Evidence indicates that the transport of molecules involved in redox metabolism, including reduced glutathione, might play an essential role in the cell death or survival process of lens fiber cells [20,21]. In addition, published studies also show that the entry of ROS contributes to cell death [19]. However, how the lens epithelial cells modulate oxidative stress in the lens as well as the consequent impact on redox balance is largely unknown. In our present study, we have elucidated a molecular mechanism underlying the cellular defense against oxidative stress in lens epithelial cells and the mechanistic role of Cx43 HCs in this process.

Oxidative stress is one of the major risk factors for cataracts, especially age-related cataracts. Studies have shown that the incidence of cataracts is higher in environments with a relatively higher ultraviolet index [45,46]. In addition, elevated H_2O_2 level is seen in the lens and aqueous humor of cataract patients. H_2O_2 at the concentration ranges found in cataracts, can cause lens opacification and produce a similar oxidation pattern to that found in cataracts, such as crystallin damage [2]. Constant exposure to UV radiation and elevated H_2O_2 level in the surrounding environment are two major sources of oxidative stress in the lens. In this study, we used both H_2O_2 and UV radiation to introduce oxidative stress in lens epithelial cells. Previous studies have shown that H_2O_2 and cigarette smoke extract can induce Cx HC opening [19]. Additionally, we have previously shown that H_2O_2 induces HC opening in bone osteocytes and lens fiber cells [20,47]. Here we observed that Cx43 HCs open temporarily in response to H_2O_2-induced oxidative stress in lens epithelial cells. Further, this opening could be inhibited by a Cx43E2 blocking antibody, which demonstrated the responsiveness of Cx43 HCs to oxidative stress. In addition to H_2O_2, another major source of oxidative insults for the lens is UV radiation. The UVR, which can be divided into three regions in increasing order of wavelengths, including UVC (100–280 nm), UVB (280–315 nm), and UVA (315–400 nm) [45]. Among these, UVB is responsible for photochemical reactions that damage the lens through the generation of ROS [48–51]. Previous studies have shown that gap junction channels respond to UV radiation. It is also reported that UV radiation affects Cx43 phosphorylation status and regulates Cx channel activity [52–55]. However, there is no direct evidence showing whether and how Cx HCs respond to UV radiation in the lens. In this study, we show that HCs open in response to UVB radiation in lens epithelial cells and the extent of the opening induced by UVB radiation is similar to that induced by H_2O_2. The activation of HCs is temporal within a limited time period. HC opening ultimately helps mitigate the elevated intracellular ROS levels induced by oxidative stress induced by either H_2O_2 or UVB. Moreover, HC activity is subjected to the regulation of the redox state of the cell.

Lens epithelial cell apoptosis is a major cause leading to initiation of non-congenital cataract formation, which is associated with intracellular accumulation of ROS [3,56]. Previous studies have shown that biphasic, protective, or detrimental roles of Cx43 channels in modulating oxidative stress-induced cell damage [20,47,57–62]. We determined the extent of oxidative stress in the lens of heterozygous Cx43 knockout mice and found that two of the major anti-oxidative enzymes, SOD1 and GPX1, were significantly reduced in the anterior epithelium, indicating the anti-oxidative role of Cx43 in anterior epithelial cells. Moreover, we found increased susceptibility to cataracts in heterozygous Cx43 knockout mice under oxidative stress compared to WT lens. Previous studies reported that $Cx43^{+/-}$ heterozygous mice do not exhibit many abnormal phenotypes as compared to WT mice and the reports on cardiac electrophysiological abnormalities are contradictory [63]. We cannot exclude the possible involvement of other tissues, but given that lens is an avascular organ, any impact due to systematic changes is unlikely to be significant.

Here we used two major oxidative insults to the lens, H_2O_2 and UVB radiation, to assess the role of Cx43 HCs in cellular oxidative damage and apoptotic cell death. In both models, we found an initial increase in redox status. This increase was quickly restored back to a normal level, indicating the strong capability of ROS scavenging and detoxification in lens epithelial cells in response to oxidative stress. This observation supports a previous notion that the lens epithelial cells are the major site in the synthesis of detoxification substances and an active glutathione redox cycle [1,24]. However, this self-recovery capability is abrogated with the inhibition of Cx43 HCs. Lens epithelial cells have a *de novo* GSH synthesis machinery associated with an unusually high concentration of reduced GSH (64 μmol per gram of wet weight) [64]. GSH from circulating and aqueous sulfur amino acids only represent a minor portion of GSH in the epithelial cells [41]. Previous studies also show that lens epithelial cells can take up circulating GSH from the aqueous humor [42,65]. Together, these reports suggest that lens epithelial cells produce endogenous GSH and uptake exogenous GSH to maintain their own redox homeostasis. We found that in the absence of extracellular GSH, GSH was regenerated *de novo* in lens following initial oxidation, consistently showing that lens epithelium is capable of generating and maintaining GSH homeostasis and cellular redox status. Inhibition of Cx43 HCs abolished this effect through elevated intracellular ROS accumulation and impaired intracellular GSH regeneration.

Cx HCs show a certain substrate selectivity and permit molecules with a molecular weight less than 1 kDa to pass through [66]. These channels mediate the exchange of small molecules between cells and the extracellular microenvironment. We show here that HCs are involved in the elevated intracellular H_2O_2 response to exogenous H_2O_2 and the efflux of ROS produced by UVB. GSSG can be regenerated into GSH through enzymatic action. A recent study reported that the permeation of GSSG in Cx46 and Cx50 HCs was extremely low [21]. In contrast, we show that Cx43 HCs are permeable to GSSG with the treatment of H_2O_2 or UVB radiation. Compared to UVB, exogenous H_2O_2 led to a short spike of intracellular H_2O_2 level and corresponding ROS. This is possibly caused by an import of H_2O_2 mediated by Cx43 HCs in lens epithelial cells; given that such a spike was not observed with the inhibition of HCs. However, we did not observe a rapid increase of ROS at 30 min time point, implying a potential indirect mechanism. Cx43 HCs are known to mediate Ca^{2+} entry into the cell. As previously reported [73], H_2O_2 triggers the entry of extracellular Ca^{2+} into the cell and promotes ROS production. We showed that inhibition of HCs impedes ROS production and this impediment of ROS could be caused by the inhibition of HC-triggered entry of Ca^{2+}. The elevation of ROS at later time points with impaired HCs is possibly a result of the impeded entry of GSH and release of GSSG. UVB, on the other hand, promotes mitochondria ROS production by complex III and complex I [74]. The production of ROS is triggered by intracellular Ca^{2+}, in contrast to extracellular Ca^{2+} entry by H_2O_2. Blockade of Cx43 HCs will likely inhibit the entry of GSH and the release of GSSG, and consequently increase ROS production.

H_2O_2 is capable of regulating redox status via the control of anti-oxidative enzymatic activity or transcription of genes encoding antioxidant enzymes [67,68]. Therefore, the transient increase of intracellular H_2O_2 in lens epithelial cells likely up-regulates transcription factors and consequently, anti-oxidative gene expression [68]. Indeed, we show that inhibition of Cx43 HCs abolished the increased expression of anti-oxidative genes, further supporting the notion that anti-oxidative genes can be regulated by intracellular H_2O_2 uptake via HCs. Interestingly, compared to that of H_2O_2, we observed an opposite response of anti-oxidative genes to UVB-induced oxidative stress. H_2O_2 is considered

a more suitable messenger to deliver redox signals from its generation site to the target site [67–69]. The superoxide anion ($O_2^{\bullet-}$) is thought to be the starting material for the production of a suite of reactive species [70]. Under UVB, photosensitive molecules subsequently react with oxygen, resulting in the generation of ROS including $O_2^{\bullet-}$, which can be converted to electric neutral H_2O_2, and further photolysis of H_2O_2 generates 2X $^{\bullet}$OH, which all contribute to the overall pro-oxidant state [36]. Thus, the major difference is that UVB induces cells to directly generate $O_2^{\bullet-}$, but not H_2O_2. The superoxide generated by UVB, unlike H_2O_2, cannot directly activate anti-oxidative gene transcription, thereby causing a delayed response compared to the activation induced by intracellular H_2O_2 transported by Cx43 HCs. In addition to the generation of ROS, UVB contributes to direct DNA damage through photo-oxidation [33], resulting in decreased gene transcription. This may lead to the downregulation of anti-oxidative genes/proteins in cells exposed to UVR and the attenuation effect seen with the inhibition of Cx43 HCs. It is worth noting that besides H_2O_2, Cx43 HCs also contribute to the transport of other types of redox-related molecules, including GSH/GSSG, which could also affect the expression of anti-oxidative stress genes. Our findings imply a protective regulation of Cx43 HCs in oxidative damage induced by UVB, likely through the temporal opening of HCs that facilitates the exchanging of redox metabolic molecules between the intracellular and extracellular environments.

How does oxidative stress induce HC opening? In addition to Cx phosphorylation, cellular redox potential regulates the gating and permeability of Cx43 HCs [28,29,71]. Contreras et al. (2002) reported that Trolox (a free radical scavenger) and DTT are efficient at reducing the ethidium bromide uptake of Cx43 HCs induced by metabolic inhibition [71]. This indicated that the permeability of Cx43 HCs was decreased by reducing agents and this decrease was not observed in cells pre-incubated with GSH (a membrane-impermeable reductant). Considering that the major effect of UVR is exerted through photochemical generation of ROS, we hypothesized that the cellular redox state was involved in the opening of Cx43 HCs induced by UVR. Our study shows that HC opening in response to UVB radiation is blocked in cells treated with membrane permeable DTT (added before and after exposure to UVB radiation) or membrane impermeable GSH (added after exposure to UVB radiation), but not in cells treated with GSH before exposure to UVB radiation. Our findings are in accordance with the work performed by Retamal et al. [28], showing that HC opening induced by metabolic inhibition can be suppressed by loading DTT in astrocytes. Our data support the involvement of the intracellular, but not extracellular, reducing environment in HC opening in response to UVB, and supporting the transport of GSH through Cx43 HCs.

Cysteine is a redox sensory amino acid residue of proteins [72]. Cytoplasmic cysteines (Cys) in Cx43 are located at the C-terminus. A previous study showed that Cys271 might be a candidate as a redox sensor since this Cys is modified by S-nitrosylation in Cx43-forming gap junction channels in endothelial cells [27]. However, until now, there was no evidence showing which Cys residues were responsible for channel activity under oxidative stress. Here we introduced mutation at the potential residues in the Cx43 C-terminus, C260A, C271A, and C298A. Our results, for the first time, show that the position C260, but not C271 and C298, is an oxidative sensor that mediates UVR-induced HC opening.

We demonstrated the presence of Cx43 functional HCs in human lens epithelial cells, and that these channels protect cells against oxidative stress and cell death. The observed protective effect is likely due to the ability of Cx43 HCs to allow H_2O_2, GSH, and GSSG passage, which is essential for maintaining cellular redox homeostasis. We further identified the C260 residue in Cx43 as a major redox sensor. Together, our findings advance the knowledge regarding the important role of Cx HCs in regulating cellular redox potential, and provide mechanistic insights into redox-related pathologies in the lens and other organs.

4. Materials and Methods

Materials. HLE-B3 cells were purchased from American Type Culture Collection (ATCC, Rockville MD, USA). HeLa cells expressing pIRES2-EGFP-Cx43 WT or HC-impaired mutants were previously generated by our laboratory. The Cx43E2 antibody was developed in our laboratory, targeting the second extracellular loop domain of Cx43. This antibody was affinity-purified and used for blocking HC function as previously described [37]. Rabbit anti-Cx43 C-terminus (CT) was developed in our laboratory. Rabbit anti-SOD1 antibody and mouse anti-GPX1/2 antibody were obtained from Santa Cruz (Dallas, TX, USA). Cx43 small interfering RNA (siRNA) and Silencer™ Negative Control were purchased from Ambion (Life Technologies, Carlsbad, CA, USA). High-capacity RNA-to-cDNA kit and Maxima SYBR Green/ROX qPCR Master Mix kit were obtained from Fisher Scientific. All other chemicals were obtained from either Sigma-Aldrich (St. Louis, MO, USA) or Thermo Fisher Scientific (Waltham, MA, USA).

Generation of heterozygous Cx43-null mice. All mice were maintained and studied in accordance with the NIH Guidelines for the Care and Use of Laboratory Animals. The animal protocols were approved by the University of Texas Health Science Center at San Antonio (UTSHSA) Institutional Animal Care and Use Committee (IACUC). The heterozygous Cx43-null mice were kindly provided by Roberto Civitelli at Washington University School of Medicine, and generated by crossing C57BL/6 Cx43 (+/+) mice with C57BL/6 Cx43 (+/−) mice. Genotyping was performed by PCR technique using genomic DNA isolated from mouse tails and corresponding primers synthesized by Integrated DNA Technologies (Coralville, IA).

Lenses tissue isolation. A small incision on the eyeball at the side of optic nerve was made to remove the lens operated under a dissection microscope. Isolated lenses were cultured in Medium 199 containing 10% FBS and 1% penicillin/streptomycin and incubated for 24 h at 37 °C. The lenses were examined to confirm their intactness and transparency throughout the entire procedure before treatment. Photographic images of lenses were acquired using a dissecting microscope.

Cell culture. HLE-B3 cells were cultured in Eagle's Minimum Essential Medium (EMEM, ATCC, Rockville MD, USA) containing 20% fetal bovine serum (FBS, Hyclone Laboratories, Logan, UT, USA) and penicillin/streptomycin (Invitrogen, Carlsbad, CA, USA) in an incubator supplied with 5% CO_2 at 37 °C. HeLa cells were cultured in Dulbecco's Modified Eagle Medium (DMEM, Invitrogen, Carlsbad, CA, USA) containing 10% FBS and 1% penicillin/streptomycin in an incubator supplied with 5% CO_2 at 37 °C. Transfected HeLa cells were selected with Geneticin™ Selective Antibiotic (G418 Sulfate, Life Technologies, Carlsbad, CA, USA) at the concentration of 1 mg/ml for 1 month. To maintain stability of expression of Cx43, 0.5 mg/ml of G418 Sulfate were applied during cell culturing.

siRNA transfection. HLE-B3 cells were transfected with 30 nM Silencer™ Negative Control or Cx43 siRNA using Lipofectamine RNAiMAX transfection reagent (Invitrogen, Carlsbad, CA, USA) according to the manufacturer instructions. 48 h after transfection, cells were treated with H_2O_2 or UVB radiation for further experiments.

Preparation of crude cell and membrane extracts, and western blot. Confluent cells were lysed and homogenized with ice-cold lysis buffer (5 mM Tris, 5 mM EDTA, and 5 mM EGTA) containing proteinase inhibitors (5 mM NEM, 2 mM PMSF, 1 mM Na_3VO_4, and 0.2 mM leupeptin). The whole cell lysate was boiled in 0.6% SDS or used to prepare crude membrane extracts. For preparation of membrane extracts, whole cell lysate was homogenized by passing through a 20G needle and centrifuged for 5 min at 1000 rpm to remove cell debris. The supernatant was then subjected to centrifugation at 45,000 rpm for 30 min (TLA55 rotor, Beckman Coulter, Brea, CA, USA) at 4 °C. The crude membrane extract pellets were resuspended in lysis buffer containing protease inhibitors, and then boiled in 1% SDS. The protein amount in whole cell lysates and membrane extracts was quantified using the microBCA assay (Pierce, Rockford, IL, USA) and equal amounts of proteins was loaded on

SDS-PAGE gel.

Primary antibodies and dilutions used in this study were as follows: Anti-Cx43CT (1:300 dilution), anti-GPX1/2 (1:100 dilution, Santa Cruz Biotechnology) and anti-SOD1 (1:300 dilution Santa Cruz Biotechnology). Primary antibodies were detected with goat anti-rabbit IgG conjugated IRDye® 800CW or goat anti-mouse IgG conjugated IRDye® 680RD (1:15,000 dilution) using a Licor Odyssey Infrared Imager (Lincoln, NE, USA). The intensity of the bands on western blots was quantified.

Immunofluorescence. The cells were seeded in a glass coverslip for 3 days, rinsed with PBS and fixed with 2% paraformaldehyde (PFA) for 10 min at room temperature (RT). The cells were washed in PBS three times, incubated in blocking buffer (2% donkey serum, 2% gelatin, 0.25% Triton X100, and 1% bovine serum albumin) for 1 h at RT, then incubated with primary antibody overnight at 4 °C, and followed by incubation with fluorescein-conjugated secondary antibody for 2 h at RT. The cells were washed with PBST three times and incubated with 4′, 6-diamidino-2-phenylindole (DAPI) for 5 min at RT. The coverslip was mounted to a slide using Fluoromount-G (SouthernBiotech, Birmingham, AL, USA) and subjected to fluorescence imaging analysis using a fluorescence microscope (Keyence BZ-X710) at DAPI and GFP filters.

Lens frozen tissue sectioning and immunofluorescence. The dissected mouse eyeballs were kept in PBS and a small incision was made using a needle (BD Lo-Dose U-100 Insulin Syringes). The entire eyeball was then fixed in 0.75% PFA for 24 h at RT, dehydrated with various concentrations of sucrose solution sequentially: first in 10% for 1 h, next in 20% for 1 h and finally in 30% at 4 °C overnight, and embedded in OCT compound (Sakura, Torrance, CA, USA). Sagittal sections (14 μm) collected were stained with primary antibodies overnight at 4 °C, and followed by incubation with fluorescein-conjugated secondary antibody for 1 h at RT and DAPI for 5 min at RT. After rinsing with PBS for three times, a drop of mounting medium was added before being covered by coverslips. The images of specimens were taken by a fluorescence microscope (Keyence BZ-X710) and the acquisition settings were kept consistent for all samples.

qRT-PCR analysis. RNAs were isolated using TRIzol Reagent (Molecular Research Center, Cincinnati, OH, USA) from various treated cells. cDNA was generated using the High-Capacity RNA-to-cDNA Kit (Applied Biosystems®, Life Technologies, Carlsbad, CA) according to the manufacturer instructions. qPCR was performed using an ABI 7900 PCR device (Applied Biosystems®, Life Technologies, Carlsbad, CA) with Maxima SYBR Green/ROX qPCR Master Mix (2X) and a two-step PCR protocol (95 °C, 10 s and 60 °C, 30 s). The primer sequences for GPX1, GPX8, GSR, GSTM2, MGST1, SOD1, and HMOX1 are provided in Table 1. 18S rRNA was used as a housekeeping gene control.

Dye uptake assay. HLE-B3 cells were grown to 85% confluency, starved for 48 h, and then subjected to H_2O_2 or UVB radiation. The cells were then incubated with 0.1 mM EtBr and 1 mg/ml fluorescein-dextran in HBSS for 5 min. Ethidium bromide (EtBr, Mr ~394 Da) was used as a tracer for HC activity. Fluorescein-dextran (Mr ~ 10 kDa), which could be taken up by dying cells but cannot pass through HCs, was used to exclude dead cells. The cells were then rinsed twice with HBSS and DPBS, respectively, fixed with 2% PFA for 10 min at RT, and subject to fluorescence imaging analysis.

HeLa cells transfected with Cx43 WT or mutants were grown to 85% confluency and starved for 48 h before UVB radiation. The cells were then treated with 0.1 mM DAPI (Mr ~ 277 Da) and 1 mg/ml rhodamine-dextran (Mr ~ 10 kDa) dye mixture HBSS for 5 min, followed by rinsing twice with HBSS and PBS, respectively, fixing with 2% PFA for 10 min at RT, and being subjected to fluorescence imaging analysis. At least three fields in a well of 12 well plates were taken using a fluorescence microscope (Keyence BZ-X710). In each field, the average pixel density of 30 random HLE-B3 cells (excluding fluorescein-dextran positive cells) and HeLa cells transfected with Cx43 WT or mutants (excluding rhodamine-dextran positive and Cx43 positive cells) were measured using a NIH ImageJ software (Bethesda, MD).

Measurement of cellular ROS and GSH. Intracellular ROS or GSH levels in cells was determined by fluorescence-based probes Carboxy-H_2DCFDA (Invitrogen, Carlsbad, CA, USA) or ThiolTracker™ (Thermo Fisher, Waltham, MA, USA) in live cells. Cells were rinsed with HBSS and incubated with 10 μM Carboxy-H_2DCFDA or ThiolTracker™ for 30 min at 37 °C. The cells incubated with Carboxy-H_2DCFDA were rinsed and maintained in HBSS and immediately followed by fluorescence imaging analysis. The cells incubated with ThiolTracker™ were rinsed twice with HBSS, fixed with 2% PFA, and were then subjected to fluorescence imaging analysis (Keyence BZ-X710). At least three fields in each well of 12-well plates were captured, and the average pixel density of 30 random cells from each field was measured using a NIH ImageJ software.

H_2O_2 uptake assay. Cells were pre-treated with Cx43E2 antibody for 30 min before the treatment with 0.3 mM H_2O_2. After H_2O_2 treatment, the cells were rinsed with HBSS and incubated with 10 μM Fluorescent Peroxide Sensor (Sigma-Aldrich, St. Louis, MO) for 8 min at 37 °C. One field was taken for each well of 96-well plates using a fluorescence microscope (Keyence BZ-X710). The intracellular H_2O_2 level was measured and quantified by determining the fluorescence intensity using the NIH ImageJ software.

Determination of GSSG. Cells were harvested by trypsinization, washed once with ice-cold DPBS, resuspended in PBS containing 0.5% NP-40, pH 6.0, and homogenized by pipetting. Proteins were removed by precipitation with trichloroacetic acid (TCA)/NaHCO3 and centrifugation at 12,000×*g*. GSH and total glutathione in the supernatant were measured in clear flat bottom black 96-well plates using the GSH/GSSG Ratio Detection Assay Kit (Abcam, Cambridge, United Kingdom) according to the manufacturer instructions. GSSG concentration was calculated as follows: GSSG = (Total glutathione – GSH)/2.

GSH uptake assay. We determined GSH transport by performing a dynamic uptake measurement using ThiolTracker™ (ThermoFisher) in live cells. Cells were pre-incubated with 1 mM GSH for 20 min before the treatment with H_2O_2 or UVB radiation with or without Cx43E2 antibody. The cells were then rinsed with HBSS and incubated with 10 μM ThiolTracker™ for 30 min. The cells were rinsed with PBS and fixed with 2% PFA. The images were taken at least three fields using a fluorescence microscope (Keyence BZ-X710). The intracellular GSH level was measured and quantified by determining fluorescence intensity using the NIH ImageJ software.

Apoptosis analysis. The cells were grown in complete culture media to 85% confluency and followed by culturing in serum-depleted media for 48 h. After being treated with H_2O_2 or UVB radiation, cells and medium were collected and centrifuged. The cell pellets were resuspended in Annexin V Binding Buffer and further processed using FITC–Annexin V Apoptosis Detection Kit (BioLegend, San Diego, CA, USA) according to the manufacturer instructions. Fluorescence images

Table 1
List of DNA primers.

Name	Sequence
GSTM2-F	5′-CCCTGAAATGCTGAAGCTCTA-3′
GSTM2-R	5′-TGGTTTCTCTCAAGGACATCATAA-3′
MGST1-F	5′-CACCCAGGTAATGGATGATGAA-3′
MGST1-R	5′-TGCTACACAGTCTTCTGGATTG-3′
GPX1-F	5′-GAATGTGGCGTCCCTCTG-3′
GPX1-R	5′-CTCTTCGTTCTTGGCGTTCT-3′
GPX8-F	5′-TCTGAAGGAGAACCTGCATTTA-3′
GPX8-R	5′-CCCTCAGGGTTGACAAGATAC-3′
SOD1-F	5′-GTGCAGGGCATCATCAATTTC-3′
SOD1-R	5′-GGCCTTCAGTCAGTCCTTTAAT-3′
HMOX1 –F	5′-TCAGGCAGAGGGTGATAGAA-3′
HMOX1 –R	5′-GCTCCTGCAACTCCTCAAA-3′
GR-F	5′-CGGTGCCAGCTTAGGAATAA-3′
GR-R	5′-GCCATCTCCACAGCAATGTA-3′
18S rRNA-F	5′-ACAGGTCTGTGATGCCCTTAGA-3′
18S rRNA-R	5′-GCAAGCTTATGACCCGCACTTA-3′

were taken by using Countess™ cell counting chamber slides using a fluorescence microscope (Keyence BZ-X710), and the percentage of positive staining cells was quantified.

Cell viability assay. The cells were grown to 85% confluency and starved for 48 h, trypsinized, centrifuged, and resuspended in PBS containing 0.4% Trypan blue. The number of viable cells and total cells were counted using a Countess II FL Automated Cell Counter (Invitrogen, Carlsbad, CA, USA).

Statistical Analysis. All data were analyzed with GraphPad Prism 7 software (GraphPad Software, La Jolla, CA). Multiple group comparisons were used by means of a one-way ANOVA and Tukey multiple comparison test. Two-way ANOVA and Sidak multiple comparison tests were used to compare the mean differences between two independent variables groups. The data are presented as mean ± SEM of at least three measurements. $P < 0.05$ was designated as a statistically significant difference. Hashtag in all figures indicated the significant differences compared between two independent variables groups. Asterisks in all figures indicate the degree of significant differences compared to controls: *, $P < 0.05$; **, $P < 0.01$; ***$P < 0.001$; ****, $P < 0.0001$.

Declaration of interest

Declarations of interest for all authors: none.

Acknowledgments

The authors thank Dr. Roberto Civitelli at the Washington University School of Medicine for generously providing Cx43 (±) mice. Dr. Eduardo R. Cardenas for proofreading and editing. The study was supported by NIH RO1 EY012085 and Welch Foundation grant AQ-1507 to J.X.J.

Appendix A. Supplementary data

Supplementary data to this article can be found online at https://doi.org/10.1016/j.redox.2021.102102.

References

[1] V.M. Berthoud, E.C. Beyer, Oxidative stress, lens gap junctions, and cataracts, Antioxidants Redox Signal. 11 (2) (2009) 339–353.
[2] A. Spector, Oxidative stress-induced cataract: mechanism of action, Faseb. J. 9 (12) (1995) 1173–1182.
[3] W.C. Li, et al., Lens epithelial cell apoptosis appears to be a common cellular basis for non-congenital cataract development in humans and animals, J. Cell Biol. 130 (1) (1995) 169–181.
[4] Y. Tamada, et al., Evidence for apoptosis in the selenite rat model of cataract, Biochem. Biophys. Res. Commun. 275 (2) (2000) 300–306.
[5] R.T. Mathias, J. Kistler, P. Donaldson, The lens circulation, J. Membr. Biol. 216 (1) (2007) 1–16.
[6] D.A. Goodenough, D.L. Paul, Beyond the gap: functions of unpaired connexon channels, Nat. Rev. Mol. Cell Biol. 4 (4) (2003) 285–294.
[7] N. Wang, et al., Paracrine signaling through plasma membrane hemichannels, Biochim. Biophys. Acta 1828 (1) (2013) 35–50.
[8] S. Burra, J.X. Jiang, Regulation of cellular function by connexin hemichannels, International journal of biochemistry and molecular biology 2 (2) (2011) 119–128.
[9] D.A. Goodenough, D.L. Paul, Gap junctions, Cold Spring Harb Perspect Biol 1 (1) (2009), a002576.
[10] E.C. Beyer, L. Ebihara, V.M. Berthoud, Connexin mutants and cataracts, Front. Pharmacol. 4 (2013) 43.
[11] X. Gong, et al., Disruption of alpha3 connexin gene leads to proteolysis and cataractogenesis in mice, Cell 91 (6) (1997) 833–843.
[12] W.A. Paznekas, et al., Connexin 43 (GJA1) mutations cause the pleiotropic phenotype of oculodentodigital dysplasia, Am. J. Hum. Genet. 72 (2) (2003) 408–418.
[13] A. Lai, et al., Oculodentodigital dysplasia connexin43 mutations result in non-functional connexin hemichannels and gap junctions in C6 glioma cells, J. Cell Sci. 119 (Pt 3) (2006) 532–541.
[14] R.J. Truscott, Age-related nuclear cataract-oxidation is the key, Exp. Eye Res. 80 (5) (2005) 709–725.
[15] M. Nita, A. Grzybowski, The role of the reactive oxygen species and oxidative stress in the pathomechanism of the age-related ocular diseases and other pathologies of the anterior and posterior eye segments in adults, Oxid Med Cell Longev 2016 (2016) 3164734.
[16] V.N. Reddy, Glutathione and its function in the lens–an overview, Exp. Eye Res. 50 (6) (1990) 771–778.
[17] M.F. Lou, Thiol regulation in the lens, J. Ocul. Pharmacol. Therapeut. 16 (2) (2000) 137–148.
[18] X. Fan, V.M. Monnier, J. Whitson, Lens glutathione homeostasis: discrepancies and gaps in knowledge standing in the way of novel therapeutic approaches, Exp. Eye Res. 156 (2017) 103–111.
[19] S. Ramachandran, L.H. Xie, S.A. John, S. Subramaniam, R. Lal, A novel role for connexin hemichannel in oxidative stress and smoking-induced cell injury, PloS One 2 (2007), e712.
[20] W. Shi, M.A. Riquelme, S. Gu, J.X. Jiang, Connexin hemichannels mediate glutathione transport and protect lens fiber cells from oxidative stress, J. Cell Sci. 131 (6) (2018).
[21] N. Slavi, et al., Connexin 46 (cx46) gap junctions provide a pathway for the delivery of glutathione to the lens nucleus, J. Biol. Chem. 289 (47) (2014) 32694–32702.
[22] M.H. Stridh, M. Tranberg, S.G. Weber, F. Blomstrand, M. Sandberg, Stimulated efflux of amino acids and glutathione from cultured hippocampal slices by omission of extracellular calcium: likely involvement of connexin hemichannels, J. Biol. Chem. 283 (2008) 10347–10356.
[23] X. Tong, et al., Glutathione release through connexin hemichannels: implications for chemical modification of pores permeable to large molecules, J. Gen. Physiol. 146 (3) (2015) 245–254.
[24] F.J. Giblin, Glutathione: a vital lens antioxidant, J. Ocul. Pharmacol. Therapeut. 16 (2) (2000) 121–135.
[25] N.M. Kumar, N.B. Gilula, The gap junction communication channel, Cell 84 (3) (1996) 381–388.
[26] S.R. Johnstone, M. Billaud, A.W. Lohman, E.P. Taddeo, B.E. Isakson, Posttranslational modifications in connexins and pannexins, J. Membr. Biol. 245 (5–6) (2012) 319–332.
[27] M.A. Lillo, et al., S-nitrosylation of connexin43 hemichannels elicits cardiac stress-induced arrhythmias in Duchenne muscular dystrophy mice, JCI Insight 4 (24) (2019).
[28] M.A. Retamal, C.J. Cort,s, L. Reuss, M.V. Bennett, J. S ez, S-nitrosylation and permeation through connexin 43 hemichannels in astrocytes: induction by oxidant stress and reversal by reducing agents, Proc.Nat.Acad.Sci.(USA) 103 (2006) 4475–4480.
[29] M.A. Retamal, K.A. Schalper, K.F. Shoji, M.V. Bennett, J.C. Saez, Opening of connexin 43 hemichannels is increased by lowering intracellular redox potential, Proc. Natl. Acad. Sci. U. S. A. 104 (20) (2007) 8322–8327.
[30] M.A. Retamal, Connexin and Pannexin hemichannels are regulated by redox potential, Front. Physiol. 5 (2014) 80.
[31] K. Pogoda, P. Kameritsch, M.A. Retamal, J.L. Vega, Regulation of gap junction channels and hemichannels by phosphorylation and redox changes: a revision, BMC Cell Biol. 17 (Suppl 1) (2016) 11.
[32] A. Kawano, et al., Autocrine regulation of UVA-induced IL-6 production via release of ATP and activation of P2Y receptors, PloS One 10 (6) (2015), e0127919.
[33] I.V. Ivanov, T. Mappes, P. Schaupp, C. Lappe, S. Wahl, Ultraviolet radiation oxidative stress affects eye health, J. Biophot. 11 (7) (2018), e201700377.
[34] F. Kamari, et al., Phototoxicity of environmental radiations in human lens: revisiting the pathogenesis of UV-induced cataract, Graefes Arch. Clin. Exp. Ophthalmol. 257 (10) (2019) 2065–2077.
[35] S.D. Varma, V.K. Srivastava, R.D. Richards, Photoperoxidation in lens and cataract formation: preventive role of superoxide dismutase, catalase and vitamin C, Ophthalmic Res. 14 (3) (1982) 167–175.
[36] J. Wenk, et al., UV-induced oxidative stress and photoaging, Curr. Probl. Dermatol. 29 (2001) 83–94.
[37] A.J. Siller-Jackson, et al., Adaptation of connexin 43-hemichannel prostaglandin release to mechanical loading, J. Biol. Chem. 283 (2008) 26374–26382.
[38] S. Bassnett, D.C. Beebe, Coincident loss of mitochondria and nuclei during lens fiber cell differentiation, Dev. Dynam. 194 (2) (1992) 85–93.
[39] H.J. Forman, H. Zhang, A. Rinna, Glutathione: overview of its protective roles, measurement, and biosynthesis, Mol. Aspect. Med. 30 (1–2) (2009) 1–12.
[40] M. Goel, R.G. Picciani, R.K. Lee, S.K. Bhattacharya, Aqueous humor dynamics: a review, Open Ophthalmol. J. 4 (2010) 52–59.
[41] J.B. Mackic, R. Kannan, N. Kaplowitz, B.V. Zlokovic, Low de novo glutathione synthesis from circulating sulfur amino acids in the lens epithelium, Exp. Eye Res. 64 (4) (1997) 615–626.
[42] J.B. Mackic, et al., Transport of circulating reduced glutathione at the basolateral side of the anterior lens epithelium: physiologic importance and manipulations, Exp. Eye Res. 62 (1) (1996) 29–37.
[43] M.A. Retamal, et al., Extracellular cysteine in connexins: role as redox sensors, Front. Physiol. 7 (2016) 1.
[44] R.T. Mathias, J.L. Rae, G.J. Baldo, Physiological properties of the normal lens, Physiol. Rev. 77 (1) (1997) 21–50.
[45] S.D. Varma, S. Kovtun, K.R. Hegde, Role of ultraviolet irradiation and oxidative stress in cataract formation-medical prevention by nutritional antioxidants and metabolic agonists, Eye Contact Lens 37 (4) (2011) 233–245.
[46] C. Delcourt, et al., Light exposure and the risk of cortical, nuclear, and posterior subcapsular cataracts: the Pathologies Oculaires Liees a l'Age (POLA) study, Arch. Ophthalmol. 118 (3) (2000) 385–392.
[47] R. Kar, M.A. Riquelme, S. Werner, J.X. Jiang, Connexin 43 channels protect osteocytes against oxidative stress-induced cell death, J. Bone Miner. Res. : the official journal of the American Society for Bone and Mineral Research 28 (7) (2013) 1611–1621.

[48] S. Lerman, Lens proteins and fluorescence, Isr. J. Med. Sci. 8 (8) (1972) 1583–1589.
[49] S. Lerman, Characterization of the insoluble protein fraction in the ocular lens, Can. J. Biochem. 47 (12) (1969) 1115–1119.
[50] J. Dillon, UV-B as a pro-aging and pro-cataract factor, Doc. Ophthalmol. 88 (3–4) (1994) 339–344.
[51] C.S. Rogers, et al., The effects of sub-solar levels of UV-A and UV-B on rabbit corneal and lens epithelial cells, Exp. Eye Res. 78 (5) (2004) 1007–1014.
[52] N. Provost, M. Moreau, A. Leturque, C. Nizard, Ultraviolet A radiation transiently disrupts gap junctional communication in human keratinocytes, Am. J. Physiol. Cell Physiol. 284 (1) (2003) C51–C59.
[53] J.H. Lin, et al., Connexin mediates gap junction-independent resistance to cellular injury, J. Neurosci. 23 (2) (2003) 430–441.
[54] K. Wang, et al., Developmental truncations of connexin 50 by caspases adaptively regulate gap junctions/hemichannels and protect lens cells against ultraviolet radiation, J. Biol. Chem. 287 (19) (2012) 15786–15797.
[55] B. Bellei, et al., Ultraviolet A induced modulation of gap junctional intercellular communication by P38 MAPK activation in human keratinocytes, Exp. Dermatol. 17 (2) (2008) 115–124.
[56] S.D. Varma, D. Chand, Y.R. Sharma, J.F. Kuck Jr., R.D. Richards, Oxidative stress on lens and cataract formation: role of light and oxygen, Curr. Eye Res. 3 (1) (1984) 35–57.
[57] M.A. Retamal, et al., Cx43 hemichannels and gap junction channels in astrocytes are regulated oppositely by proinflammatory cytokines released from activated microglia, J. Neurosci. 27 (50) (2007) 13781–13792.
[58] H.T. Le, et al., Gap junction intercellular communication mediated by connexin43 in astrocytes is essential for their resistance to oxidative stress, J. Biol. Chem. 289 (3) (2014) 1345–1354.
[59] M.A. Riquelme, J.X. Jiang, Elevated intracellular Ca(2+) signals by oxidative stress activate connexin 43 hemichannels in osteocytes, Bone Res 1 (4) (2013) 355–361.
[60] C.M. Hutnik, C.E. Pocrnich, H. Liu, D.W. Laird, Q. Shao, The protective effect of functional connexin43 channels on a human epithelial cell line exposed to oxidative stress, Invest. Ophthalmol. Vis. Sci. 49 (2) (2008) 800–806.
[61] X. Fang, et al., Connexin43 hemichannels contribute to cadmium-induced oxidative stress and cell injury, Antioxidants Redox Signal. 14 (12) (2011) 2427–2439.
[62] V.A. Figueroa, et al., Contribution of connexin hemichannels to the decreases in cell viability induced by linoleic acid in the human lens epithelial cells (HLE-B3), Front. Physiol. 10 (1574) (2020).
[63] D. Eckardt, et al., Functional role of connexin43 gap junction channels in adult mouse heart assessed by inducible gene deletion, J. Mol. Cell. Cardiol. 36 (1) (2004) 101–110.
[64] F.J. Giblin, B. Chakrapani, V.N. Reddy, Glutathione and lens epithelial function, Invest. Ophthalmol. Vis. Sci. 15 (5) (1976) 381–393.
[65] B.V. Zlokovic, et al., Blood-to-lens transport of reduced glutathione in an in situ perfused Guinea-pig eye, Exp. Eye Res. 59 (4) (1994) 487–496.
[66] A.P. Quist, S.K. Rhee, H. Lin, R. Lal, Physiological role of gap-junctional hemichannels. Extracellular calcium-dependent isosmotic volume regulation, J. Cell Biol. 148 (5) (2000) 1063–1074.
[67] H. Sies, Hydrogen peroxide as a central redox signaling molecule in physiological oxidative stress: oxidative eustress, Redox Biol 11 (2017) 613–619.
[68] H.S. Marinho, C. Real, L. Cyrne, H. Soares, F. Antunes, Hydrogen peroxide sensing, signaling and regulation of transcription factors, Redox Biol 2 (2014) 535–562.
[69] H.J. Forman, M. Maiorino, F. Ursini, Signaling functions of reactive oxygen species, Biochemistry 49 (5) (2010) 835–842.
[70] A. Rahal, et al., Oxidative stress, prooxidants, and antioxidants: the interplay, BioMed Res. Int. 2014 (2014) 761264.
[71] J.E. Contreras, et al., Metabolic inhibition induces opening of unapposed connexin 43 gap junction hemichannels and reduces gap junctional communication in cortical astrocytes in culture, Proc. Natl. Acad. Sci. U. S. A. 99 (1) (2002) 495–500.
[72] L.B. Poole, The basics of thiols and cysteines in redox biology and chemistry, Free Radic. Biol. Med. 80 (2015) 148–157.
[73] H. Sies, Dean P. Jones, Reactive oxygen species (ROS) as pleiotropic physiological signalling agents, Nat. Rev. Mol. Cell Biol. 21 (2020) 363–383, https://doi.org/10.1038/s41580-020-0230-3. https://www.nature.com/articles/s41580-020-0230-3?proof=thttps%3A%2F%2Fwww.nature.com%2Farticles%2Fsj.bdj.2014.353%3Fproof%3Dt.
[74] R. Gniadecki, T. Thorn, J. Vicanova, A. Petersen, H.C. Wulf, Role of mitochondria in ultraviolet-induced oxidative stress, J. Cell Biochem. 80 (2) (2000 Oct 20) 216–222. https://onlinelibrary.wiley.com/doi/10.1002/1097-4644(20010201)80:2%3C216::AID-JCB100%3E3.0.CO;2-H.